Bulgarian Journal of Physics vol. **XX** (20XX) 1–11

Spectroscopic Investigations of Mn^{2+} Doped B_2O_3-ZnO-Bi_2O_3 Glasses

Bejjipurapu Chandrasekhar[1], **Satyanarayana Talam**[2], **Ramesh Sopinti**[2], **Nagarjuna Gunnam**[3], **Rajeswara Rao Darsi**[4], **G. Bhanu Kiran**[5], **B.V. Raghavaiah**[6*]

[1]Department of Physics, Acharya Nagarjuna University-522510, Guntur, Andhra Pradesh, India

[2]Department of ECE, Lakireddy Bali Reddy College of Engineering (Autonomous), Mylavaram-521230, NTR District, Andhra Pradesh, India

[3]Department of Chemistry, Government Degree College, Avanigadda-521121, Krishna District, Andhra Pradesh, India

[4]Department of Physics, Government Junior College, Tiruvuru-521235, Andhra Pradesh, India

[5]Department of Mechanical Engineering, RGUKT-Nuzvid Campus, Rajiv Gandhi University of Knowledge Technologies–Andhra Pradesh, Nuzvid, 521201, Andhra Pradesh, India

[6]Department of Physics, RGUKT - Ongole Campus, Rajiv Gandhi University of Knowledge Technologies-Andhra Pradesh, Ongole, 523001, Andhra Pradesh, India

*Corresponding author Email: bv_raghavaiah@rediffmail.com

Received *3 December 2024*

Abstract. A glass system of specific composition $55B_2O_3$-$20Bi_2O_3$-(25-x)ZnO: x MnO ($0.5 \leq x \leq 2.0$ mol%) was synthesized by conventional melt quenching technique. Structural, morphological, optical absorption, photoluminescence (PL) and electron paramagnetic resonance (EPR) studies were carried out on the prepared sample. The XRD pattern of the glasses revealed the amorphous nature of the samples. SEM images indicated very few crystal grains in the samples, indicating the possible occurrence of crystallization during the annealing process. Differential thermal analysis (DTA) studies indicated a down trend in the rigidity of glass network associated with glass transition temperature. The bands corresponding to divalent and trivalent manganese ions were observed in UV-visible region. The emission spectra exhibited two characteristic bands in the regions around 510–560 nm and 610–650 nm corresponding to transitions of divalent manganese ions positioned in tetrahedral and octahedral symmetries. EPR showed the characteristic resonance signals of Mn^{2+} ions in all glass samples. The factors for increasing structural degree of disorder and occupying tetragonal and octahedral symmetry changes with the content of MnO were discussed.

KEY WORDS: Mn^{3+} ions, Zinc bismuth borate glasses, Absorption, EPR, Emission.

1 Introduction

Being very good glass former and exhibiting low melting temperature, low refractive index, host material for different lasing ions and high heat resistance, borate glasses were given lot of attention by many researchers for investigations to explore their suitability to be used in optical devices [1–3]. Adding Bi_2O_3 to a borate glass network is highly expected to improve the density, refractive index, and optical properties of glass samples due to Bi_2O_3's high atomic number and polarizability. It also helps in modifying the glass structure, improving thermal stability, and potentially increasing the glass's non-linear optical properties, making it suitable for photonic applications [4–6]. More specifically, the inclusion of Bi_2O_3 in borate glass systems is known to introduce lone pair electrons, which can create non-bridging oxygens (NBOs) that influence the glass network's rigidity and optical properties. This makes the glass system versatile for applications in optoelectronics and nonlinear optics [7, 8].

ZnO acts as a network modifier, disrupting the glass structure and introducing non-bridging oxygens (NBOs), which can enhance the glass's optical transparency and alter its refractive index. ZnO also contributes to improving the chemical durability and thermal stability of the glass, making it more resistant to environmental degradation. Additionally, ZnO can influence the electronic and optical properties, making the glass suitable for various applications [9, 10].

Among all transition metal ions, manganese (Mn) ion is particularly interesting because it exists in different valence states in different glass matrices. Introducing MnO in small quantities to the ZnO-Bi_2O_3-B_2O_3 glass network can significantly impact the glass's spectroscopic properties. MnO typically exists in multiple oxidation states (Mn^{2+}, Mn^{3+}), which can act as both network modifiers and form coordination complexes within the glass matrix. This can result in distinct absorption bands in the UV-Vis and IR regions, attributed to d-d transitions and charge transfer processes involving Mn ions. The presence of MnO can also enhance the glass's luminescence properties, making it useful for applications in optical amplifiers, lasers, and other photonic devices where controlled light absorption and emission are critical [11–13]. By incorporating Bi_2O_3 alongside ZnO and MnO, the glass matrix may exhibit enhanced spectroscopic properties and improved thermal and chemical durability. These improvements are critical for developing advanced materials that can withstand extreme environments, making them suitable for high-performance optical devices and sensors [14–16]. The possible oxidation states of manganese ions like divalent and trivalent further help in modifying optical properties of boro bismuth glasses by means of occupying either tetrahedral or octahedral positions. Thus, a lot of scope is there to explore the optical features of manganese doped Bi_2O_3-B_2O_3 glasses for appropriate real time transmission applications covering a wide range of communication windows. Nevertheless, most of the studies were focused on introduction of modifier oxides in to either silicate or phosphate glass networks,

but limited investigations are there on MnO doped borate-based bismuth zinc glass network [17, 18].

Considering interesting facts about all the constituents in the proposed glass composition in addition to limited research works on role of MnO ions in this glass network environment [19–21], the present work is aimed at synthesizing, characterizing and investigating the spectral features of MnO mixed zinc bismuth borate glasses by means of structural modifications with the occurrence and occupancy of divalent and trivalent manganese ions.

2 Experimental Section

A specific glass matrix of $55B_2O_3-20Bi_2O_3$-(25-x)ZnO:x MnO was finalized after many attempts considering glass preparing zone of B_2O_3- Bi_2O_3-ZnO system. Using melt quench technique, glasses were synthesized, and samples were labelled corresponding to their glass composition given below:

$$\begin{aligned}
&\mathrm{BBZM_5}: && 55B_2O_3 - 20Bi_2O_3 - 24.5ZnO : 0.5MnO \\
&\mathrm{BBZM_{10}}: && 55B_2O_3 - 20Bi_2O_3 - 24ZnO : 1.0MnO \\
&\mathrm{BBZM_{15}}: && 55B_2O_3 - 20Bi_2O_3 - 23.5ZnO : 1.5MnO \\
&\mathrm{BBZM_{20}}: && 55B_2O - 20Bi_2O_3 - 23ZnO : 2.0MnO
\end{aligned}$$

Analytical grade raw chemicals like H_3BO_3, Bi_2O_3, $ZnCO_3$ and MnO all in mol% were taken in suitable amounts, rigorously mixed using agate mortar and piston, then obtained smooth powder transferred into a platinum crucible and kept in the furnace at around 950 to 1100°C for half an hour. Later, molten liquid formed without any bubbles is poured on to the pre-heated brass moulds to get required shapes and subsequent annealing at 350°C to make samples void free. As a regular procedure, optical polishing is done for further characterization of samples.

Using Archimedes' method, densities of all samples were measured by taking o-xylene. Glass nature was tested by Rigaku D/Max ULTIMA III X-ray diffractometer (XRD) with a CuKα radiation and surface morphology by Zeiss high resolution field emission Ultra Plus scanning electron microscope (HR FE-SEM). To carry out differential thermal studies, Netzsch Simultaneous STA409C DSC/TG Thermal Analyzer was employed. UV-3092 spectrophotometer was used to record UV-visible absorption spectra and F-2500 FL Spectrophotometer for measuring emission spectra. JEOL JES-TES100 X-band EPR spectrometer (9.4 GHz) was used to record electron paramagnetic resonance.

3 Results and Discussion

Initially, average molecular weight, manganese ion concentration N_i, mean 'Mn' ion separation r_i, polaron radius r_p [4, 10] and density are measured and pre-

Table 1. Physical parameters of B_2O_3-Bi_2O_3-ZnO:MnO glasses

Sample	Avg. Mol. Wt. (g/mol)	Density (g/cm^3)	Concentration of 'Mn' ions N_i (10^{21}/cm^3)	Interionic distance of 'Mn' ions r_i (Å)	Polaron radius r_p (Å)
$BBZM_5$	151.78	4.535	8.99	0.48	0.19
$BBZM_{10}$	151.73	4.531	17.98	0.38	0.15
$BBZM_{15}$	151.68	4.528	26.97	0.33	0.13
$BBZM_{20}$	151.63	4.524	35.94	0.30	0.12

sented in Table 1. The addition of MnO to the glass samples resulted in a slight decrease in their density, molecular weight, r_i, and r_p. This could be attributed to the fact that MnO was added to the glass network in place of ZnO, which has a more molecular weight than that of manganese oxide. As a result, the addition of MnO caused a disruption in the fundamental borate linkages in BO_4 tetrahedrons, leading to an increase in the degree of network disorder. This was further compounded by the development of cross-linkages between MnO, ZnO, $Bi_2O_3$and B_2O_3, which contributed to the extension of the degree of network disorder in the glass samples. It is important to note that the increase in manganese content also had an impact on the physical properties of the glass samples.

X-ray diffraction (XRD) is a non-destructive technique used to analyze the crystallographic structure of materials. It works by shining a beam of X-rays onto

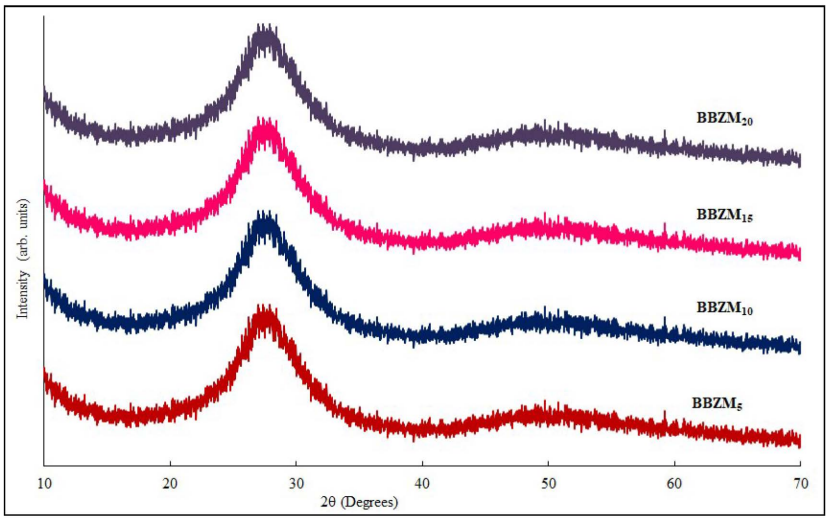

Figure 1. XRD patterns of B_2O_3-Bi_2O_3-ZnO:MnO glasses.

a sample and measuring the diffraction patterns produced as the X-rays interact with the atoms in the material. The XRD is commonly used to identify the crystal structure of a material and to determine the presence of any crystalline phases. The XRD pattern was recorded on B_2O_3-Bi_2O_3-ZnO:MnO glasses, as depicted in Figure 1. The XRD pattern of the glasses did not show any significant peaks, indicating the amorphous nature of the samples [7, 10, 22, 23]. An amorphous material lacks a long-range ordered structure and appears as a disordered solid with a broad, featureless XRD pattern. This is in contrast to crystalline materials, which exhibit sharp and distinct XRD peaks that are characteristic of their crystal structure. The lack of significant peaks in the XRD pattern of the glasses further suggests that there are no prominent crystallization possibilities during the synthesis process. The absence of XRD peaks indicates that the glasses did not undergo any such transition during the synthesis process.

Scanning electron microscopy is a technique that utilizes a focused beam of electrons to produce high-resolution images of the surface of a material. The results of scanning electron microscopy (SEM) images of $B_2O_3-Bi_2O_3$-ZnO:MnO glasses are shown in Figure 2. The SEM images revealed very few crystal grains in the samples, indicating the possible occurrence of crystallization during the annealing process. However, overall, the images validate the non-crystalline nature of the samples [7, 10]. Furthermore, the images also indicate that the glass samples did not contain any voids or cracks. The absence of voids and cracks in the SEM images suggests that the prepared glasses were synthesized under controlled conditions, with minimal defects or impurities. Annealing is a process of heating and cooling a material to alter its properties or relieve stress. In the context of glass, annealing is used to relieve stress and to prevent cracking. Despite the possible occurrence of crystallization during the annealing process, the SEM images validate the non-crystalline nature of the $B_2O_3-Bi_2O_3$-ZnO:MnO

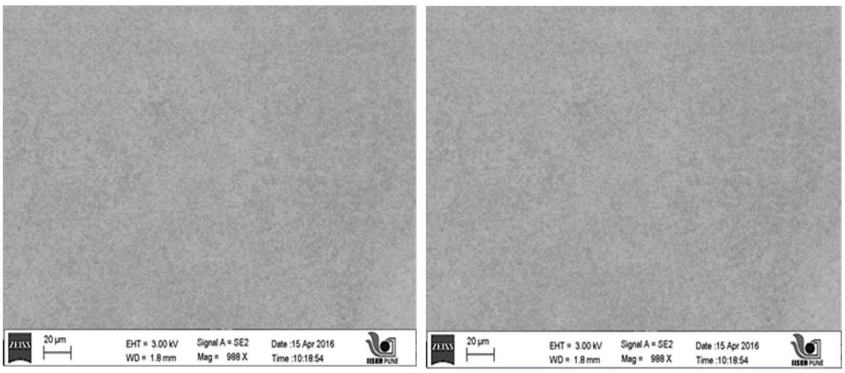

Figure 2. Scanning electron microscopic pictures of $BBZM_5$ and $BBZM_{20}$ (Left to Right).

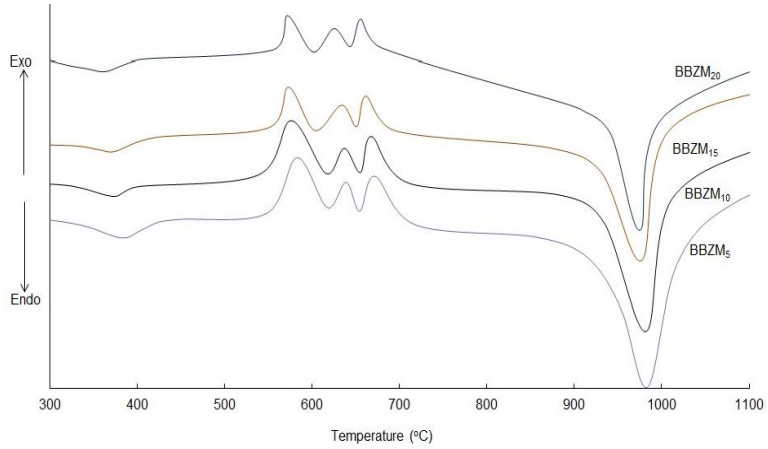

Figure 3. DTA traces of B_2O_3-Bi_2O_3-ZnO:MnO glasses.

glasses. This is because the images showed very few crystal grains in the samples, indicating that the samples are mostly amorphous in nature. The non-crystalline nature of the glasses was also confirmed by the absence of significant peaks in the X-ray diffraction pattern.

The DTA traces showed in Figure 3 are characteristic endothermic and exothermic peaks which suggest that the samples are uniform in composition. The presence of these peaks in all the samples suggests that the synthesis process was controlled and consistent. The results also indicate that the addition of MnO leads to a decrease in the glass transition temperature, and the sample $BBZM_{20}$ was found to exhibit a lower glass transition temperature than the other samples. The Mn^{2+} ions along with Zn^{2+} ions are responsible for modifying the bismuth and borate glass networks, leading to an increased number of non-bridging oxygens and more structural disorders [23–26]. This means that the addition of MnO to the glass network leads to a decrease in the temperature at which the glass undergoes a transition from a hard and brittle state to a soft and pliable state. This could have significant implications for the mechanical and spectral properties of the glasses.

UV-visible absorption spectra of MnO added B_2O_3-Bi_2O_3-ZnO glasses are depicted in Figure 4. The results showed that the absorption edges of all the samples shifted towards the red region of the spectrum with increasing MnO content. This shift is an indication of the presence of divalent manganese ions in the glass network. The spectra have exhibited three bands at 410, 435 (Td), and 534 (Oh) attributed to $^6A_{1g}(S) \rightarrow {}^4A_{1g}(G)$, $^6A_{1g}(S) \rightarrow {}^4T_{2g}(G)$ and $^6A_{1g}(S) \rightarrow {}^4T_{1g}(G)$ of divalent manganese ions [25, 26]. The Td and Oh notations indicate the point group symmetries of the vibrational modes involved in the transitions. The transitions indicate the presence of divalent manganese ions in the glass network,

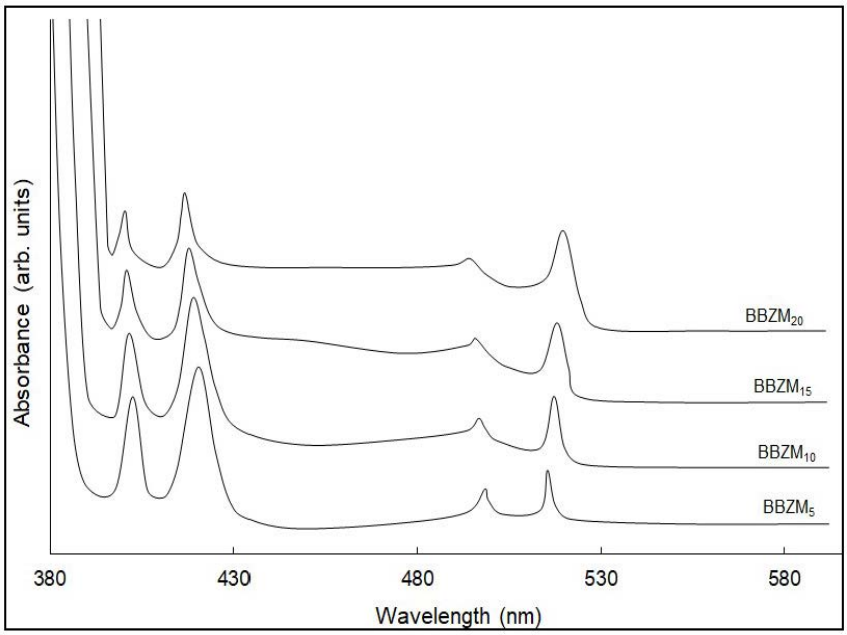

Figure 4. Optical absorption spectra of B_2O_3-Bi_2O_3-ZnO:MnO glasses.

which play a crucial role in the optical properties of the glasses. The red shift in the absorption edge is a result of the crystal field splitting caused by the Mn^{2+} ions.

As the MnO content in the glass increases, the number of Mn^{2+} ions also increase, leading to more pronounced crystal field splitting. This crystal field splitting causes the absorption edges to shift toward the red region of the spectrum.

Interestingly, a minor peak at about 495 to 505 nm was observed that could be the transition $^5E_g \rightarrow {}^5T_{2g}$ of trivalent manganese ions [23, 24]. The addition of dopants causes change in the distribution of manganese ions in the glass network. Specifically, the number of divalent manganese ions occupying tetrahedral positions decreases, while the number of octahedrally positioned Mn^{2+} ions increase. These changes in the distribution of manganese ions act as a modifier and leads enhanced degree of network disorder. This increase in network disorder is due to the presence of more non-bridging oxygen atoms, which further reduces the optical bandgap of the samples.

Additionally, the spectral analysis of the samples showed a fade-out of the peak due to the presence of Mn^{3+} ions. This is likely a result of the reduction of Mn^{3+} to Mn^{2+} during the annealing process. Furthermore, an increase in the intensity and half-width of three bands was observed, which were attributed to the transitions of the $^6A_{1g}$(S) state of the divalent manganese ions.

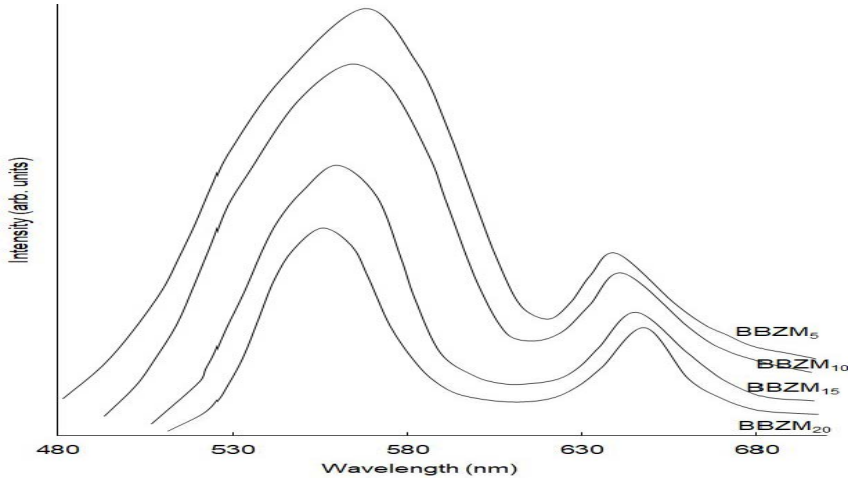

Figure 5. Emission spectra of B_2O_3-Bi_2O_3-ZnO:MnO glasses.

The photoluminescence spectra (Figure 5) of glass samples excited at their absorption edges have displayed two prominent bands; one is in the range 510 to 560 nm attributed to divalent manganese ions corresponding to transitions $^4T_{1g}(G) \rightarrow {}^6A_{1g}(S)$ of octahedrally positioned and the second one is 610 to 650 nm assigned to $^4T_1(G) \rightarrow {}^6A_1(S)$ of tetrahedrally occupied respectively [24–26]. The results of the study showed that the second band in the spectra of the glasses was fading with the addition of MnO. This suggests that the spectral properties of the glasses were changing due to the presence of MnO in the glass network. Furthermore, the first band in the spectra of the glasses was observed to be growing with the addition of MnO. This change in the intensity of the first band is associated with the decrease in the number of divalent 'Mn' ions occupying tetrahedral and octahedral positions in the glass network. Specifically, the second band in the spectra of the glasses fades with MnO addition, while the first band grows, indicating a decrease in the number of divalent 'Mn' ions occupying tetrahedral and octahedral positions in the glass network.

Electron paramagnetic resonance (Figure 6) spectra manifest two characteristic resonance signals; one is at $g = 2.02$ with hyper fine splitting corresponding to Mn^{2+} ions in octahedral positions and another is at $g = 4.3$ assigned to deformed octahedral coordinated Mn^{2+} ions, in distorted sites of octahedral symmetry [24, 26]. The analysis of the EPR spectra of the glasses showed an increasing intensity and half-width of both signals with MnO addition. This suggests that the addition of MnO to the glasses has an impact on the EPR spectra, resulting in changes in the electron spin resonance properties of the glasses. In particular, the $BBZM_{20}$ sample exhibited a strong dipolar interaction that increased the internal magnetic field around the Mn^{2+} ion. This may be one of

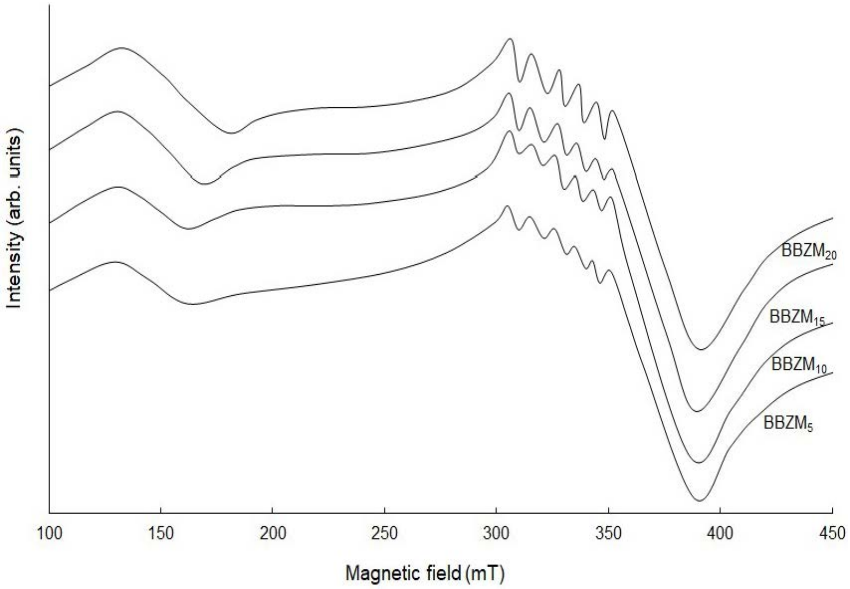

Figure 6. EPR spectra of B_2O_3-Bi_2O_3-ZnO:MnO glass samples.

the reasons for the changes in the 'g' values observed in the EPR spectra of the glasses. The bonding between manganese and oxygen ions, octahedral ligand field, orbital angular momentum, localized magnetic field, and spin-orbit interaction were identified as the key factors causing variations in the 'g' values observed in the EPR spectra of the glasses. In conclusion, the study showed that the addition of MnO to the B_2O_3-Bi_2O_3-ZnO glasses has an impact on the electron spin resonance properties of the glasses. Furthermore, the $BZZM_{20}$ sample exhibited a strong dipolar interaction that contributed to the changes in the 'g' values observed in the EPR spectra.

4 Conclusions

Mn^{2+} doped B_2O_3-Bi_2O_3-ZnO glass samples were prepared by following melt-quenching process. Increasing structural disorder was evidenced from the analyses on physical parameters. The XRD pattern of the glasses revealed the amorphous nature of the samples. SEM images indicated very few crystal grains in the samples, indicating the possible occurrence of crystallization during the annealing process. DTA traces had shown that the addition of MnO has resulted in a down trend in glass transition temperature. Optical absorption studies revealed the three characteristic absorption bands of divalent and trivalent manganese ions. Octahedrally coordinated Mn^{2+} ions increased and tetrahedrally positioned ions decreased with MnO. Red shift of the absorption edges is ob-

served. The emission spectra shown two bands in the green and red zones corresponding to $^4T_{1g}(G) \rightarrow {}^6A_{1g}(S)$ octahedrally and tetrahedrally occupied divalent manganese ions. EPR spectra presents two resonance signals; one is at $g = 2.02$ divalent manganese ions in octahedral positions; second one is at $g = 4.3$ assigned to octahedral Mn^{2+} ions.

References

[1] M.A. Marzouk, Y.M. Hamdy, H.A. Elbatal (2017) *J. Non-Cryst. Sol.* **458** 1-14.

[2] M.A. Ouis, M.A. Azooz, H.A. El Batal (2018) *J. Non-Cryst. Sol.* **494** 31-39.

[3] M. Karimi, M. Ali, M.H. Hekmatshoar, S. Vafaei (2019) *J. Non-Cryst. Sol.* **525** 119693.

[4] S. Sreehari Sastry, B. Rupa Venkateswara Rao (2014) *Physica B* **434** 159-164.

[5] P. Subbalakshmi, D.K. Durga, B. Anila Kumari, K. Srilatha (2009) *IOP Conf. Series* **2** 012023.

[6] G. Ravi Kumar, T. Srikumar, M.C. Rao, P. Venkat Reddy, Ch. Srinivasa Rao (2018) *Optik* **161** 250-265.

[7] R. Priyanka, S. Arunkumar, Ch. Basavapoornima, R. Mary, K. Marimuthu (2020) *J. Lumin.* **220** 116964.

[8] E.M.A. Hussein (2019) *J. Chem. Soc. Pak.* **41** 52.

[9] A. Abdelghany, A.H. Hammad (2015) *Spectrochim. Acta Part A Mol. Biomol. Spectrosc.* **137** 39-44.

[10] S. Talam, R. Busi, N. Gunnam, P.S. Prasad, V.R. Penugonda (2019) *J. Optoelectron. M.* **21** 530-535.

[11] K.Singh, J.Ratnam, *Solid State Ionics*, 31, 221–226 (1988).

[12] U. Issever, G. Kilic, E. Ilik (2021) *Opt. Mater.* **116** 111084.

[13] H.A.S. Al-Shamiri, A.S. Eid (2012) *Photonics and Optoelectronics* **1** 1-8.

[14] M.A. El-Ahdal, E.M. Antar, H.H. Mahmoud, F.M. Ezz-Eldin (2011) *J. App. Sci. Res.* **7** 1434-1441.

[15] S. Ruengsri (2014) *Sci. Technol. Nucl. Install.* Article ID 218041.

[16] J.D. Lee (1996) "*Concise Inorganic Chemistry*". Blackwell Scientific, Oxford.

[17] A. Van Die, A.C.H.I. Leenaers, G. Blasse, W.F. Van Der Weg (1988) *J. NonCryst. Solids* **99** 32-44.

[18] A. Margaryan, J.H. Choi, F.G. Shi (2004) *Appl. Phys. B* **78** 409-413.

[19] R.P.S. Chakradhar, K.P. Ramesh, J.L. Rao, J. Ramakrishna (2003) *J. Phys. Chem. Solids* **64** 641-650.

[20] Y. Masaru, Y. Zhidong, M. Yoshinobu, U. Yasushi, K. Kohei, Y. Tetsuo (2004) *J. Non-Cryst. Solids* **333** 37-43.

[21] L.B. Glebov, L.N. Glebova, D.E. Jones, R.R. Rakhimov (2000) *J. Non-Cryst. Solids* **265** 181-184.

[22] G. Krishna Kumari, Ch. Rama Krishna, Sk. Muntaz Begum, V. Pushpa Manjari, P.N. Murthy, R.V.S.S.N. Ravikumar (2013) *Spectrochem. Acta Mol. Biomol. Spectros.* **101** 140-147.

[23] T. Satyanarayana, M.A. Valente, G. Nagarjuna, N. Veeraiah (2013) *J. Phys. Chem. Solids* **74** 229-235.

[24] M.H. Wan, P.S. Wong, R. Hussin, H.O. Lintang, S. Endud (2015) *Spectrosc. Lett.* **48** 473-480.

[25] D.F. Franco, D. Manzani, E.E. Carvajal, G.A. Prando, J.P. Donoso, C.J. Magon, S.G. Antonio, Y.G. Gobato, M. Nalin (2020) *J. Mater. Sci.* **55** 9948-9961.

[26] M.A. Ouis, M.A. Taha, G.T. El-Bassyouni, M. Azooz (2019) *Bull. Mater. Sci.* **42** 246.